Advances in Biphoton Pulse Shaping

Joseph M. Lukens

ECE 695 Spring 2014 Term Paper,
Purdue University

Recent research has demonstrated how classical optical techniques can be extended to nonclassical entangled photon states, permitting unprecedented control of the time-frequency correlations shared by these light quanta. In this review, we discuss the theory behind such "biphoton pulse shaping" and highlight several key experiments conducted in this field. We consider both Fourier-transform pulse shaping, which relies on programmable spectral filtering, and electro-optic modulation, in which the temporal phase of the biphoton is manipulated by an electrical signal. Both avenues of research have facilitated new insights about biphoton correlations and are poised for continued advances in the near future.

I. INTRODUCTION

The groundbreaking experiments of Hanbury Brown and Twiss in the 1950s (Hanbury Brown and Twiss, 1956a,c) highlighted a grave need in the optical community to better understand the correlations shared by multiple photons. Virtually all optical interference experiments prior to that time had consisted of basic intensity measurements, whose quantum description could be understood as the interference of a single photon with itself. Yet Hanbury Brown and Twiss instead examined the correlations between *two* photoelectric detectors, finding that a pair of photons from a thermal light source are twice as more likely to arrive together than delayed, an effect now termed bunching (Chekhova, 2011). The surrounding debate (Brannen and Fergusen, 1956; Fellgett, 1957; Hanbury Brown and Twiss, 1956b; Purcell, 1956), coupled with the advent of the laser, prompted Glauber to formulate the first fully quantized field of optical coherence in 1963 (Glauber, 1963a,b), and the modern era of quantum optics was born.

Since then, a particularly influential nonclassical state of light has proven to be the entangled photon pair, or biphoton (Shih, 2003). Although such photons can be entangled in many possible degrees of freedom, in this paper our focus is on time-frequency entanglement, frequently produced through spontaneous parametric downconversion (SPDC) of a narrowband pump field, in which a single pump photon decays into two entangled photons traditionally denoted "signal" and "idler." Whereas individually these photons possess an essentially random creation time, collectively their detection times are highly correlated, since they share the same birth; likewise, their frequencies can assume any value from a potentially wide bandwidth, but once the energy of one photon is measured, the value of its partner is known with high precision. These simultaneously narrow spectro-temporal correlations violate the seemingly reasonable tenet of classical locality; although critiqued by even the likes of Einstein (Einstein *et al.*, 1935), such entanglement has proven essential in foundational tests of quantum mechanics (Aspect, 1999) and even some forms of quantum cryptography (Gisin *et al.*, 2002).

As might be expected, a key tool for characterizing biphoton entanglement derives from Glauber's coherence theory, particularly the second-order correlation function in either temporal or spectral form. Such an entangled state displays "super-bunching," for the probability of simultaneous photon detections can be radically higher than the 2:1 contrast observed for thermal light (Chekhova, 2011). And while biphoton *characterization* is certainly of great importance in itself, the last decade has also witnessed the emergence of pulse shaping techniques for biphoton *manipulation*, exploiting methods previously developed in classical ultrafast optics (Weiner, 2011). The purpose of this paper is to review these recent advances in biphoton pulse shaping, emphasizing both the impact they have already had on the field of quantum optics and their promise in future applications in quantum information. Additionally, although pulse shaping is typically associated with programmable filtering in the spectral domain to achieve shaping in time, for the purposes of this work we will also generalize the term to include its Fourier dual: modulation in the time domain to transform the spectrum. Both specializations demonstrate how classical communication techniques can find new applications in quantum optics.

In Sec. II, we provide an outline of the basic theory of biphoton shaping, followed by a discussion of photon detection methods utilized in previous experiments in Sec. III. In the case of spectral filtering in particular, observation of ultrafast temporal correlations has only been made possible through newly demonstrated nonlinear detection schemes. Section IV then covers the recent experiments conducted in this field, and in Sec. V we conclude with an outlook for future work.

II. BIPHOTON PULSE SHAPING THEORY

As noted in the introduction, SPDC of a monochromatic pump can be used to generate time-frequency entangled photons, which share both high temporal and high spectral correlation. To confirm this statement mathematically, we invoke the formalism of the interaction picture of quantum mechanics (Mandel and Wolf, 1995), in which the quantum state evolves in time according to an interaction Hamiltonian (in our case a second-order nonlinear interaction), and the field operators ac-

Typeset by REVTEX

cording to the free Hamiltonian (simply related to linear propagation of the corresponding classical fields). For a pump frequency of $2\omega_0$, a perturbative calculation (Mandel and Wolf, 1995) yields the entangled state

$$|\Psi\rangle = M|\text{vac}\rangle_s|\text{vac}\rangle_i + \int d\Omega\, \phi(\Omega)|\omega_0+\Omega\rangle_s|\omega_0-\Omega\rangle_i, \quad (1)$$

where $M \sim 1$, "vac" denotes the vacuum state, s, i signify signal and idler modes, and $\phi(\Omega)$ is a complex weight function determined by phase-matching conditions. In this form we have neglected any spatial or polarization dependencies, which prove unimportant for the experiments considered in this review. The vacuum term, with a near-unity weighting coefficient, signifies the relative improbability of this spontaneous process; downconversion efficiencies of only up to about 10^{-5} have been reported in the experiments discussed in this review (Lukens *et al.*, 2013b). Of course the more interesting term in Eq. (1) is the second one, which consists of a superposition of signal and idler photon pairs, subject to the constraint that their frequencies must sum to $2\omega_0$. Since $\phi(\Omega)$ can be extremely broadband, a wide range of frequency pairs are possible, thereby producing strong entanglement. The degree of such entanglement can be operationally defined as the ratio of the single-photon bandwidth to that conditioned on a frequency measurement of its partner (Chekhova, 2011); for a separable (non-entangled state), this value is one, whereas for an entangled state with terahertz-scale bandwidth and perhaps megahertz pump linewidth—typical for the experiments considered here—the ratio can be well over a million. Such massive entanglement lies at the heart of the nonclassical behavior which these states can display.

For the formal pulse shaping experiments, manipulation and measurement of the time-frequency entangled biphoton state follows the basic setup in Fig. 1(a). Signal and idler photons are sent through programmable spectral filters, $H_s(\omega)$ and $H_i(\omega)$, and coincidences between two detectors are measured as the signal delay is varied. Assuming the detectors are ideal—i.e., possess infinite timing resolution and respond to all frequencies of the incoming field—the coincidence rate is directly proportional to the second-order Glauber correlation function (Glauber, 1963a)

$$G^{(2)}(\tau) = \langle\Psi|\hat{E}_i^{(-)}(t)\hat{E}_s^{(-)}(t+\tau)\hat{E}_s^{(+)}(t+\tau)\hat{E}_i^{(+)}(t)|\Psi\rangle. \quad (2)$$

The positive-frequency electric field operators $\hat{E}_s^{(+)}(t+\tau)$ and $\hat{E}_i^{(+)}(t)$ are associated with annihilation of a signal or idler photon at time $t+\tau$ or t, respectively; the corresponding negative-frequency operators create photons at these times. Since the monochromatic pump is statistically stationary, the correlation function depends only on the delay τ, making the choice of t arbitrary. Moreover, because the positive- and negative-frequency operators are related through Hermitian conjugation, the classical expression for $G^{(2)}(\tau)$, in which the electric fields become simple complex numbers, is of the form of an intensity correlation between the signal and idler fields,

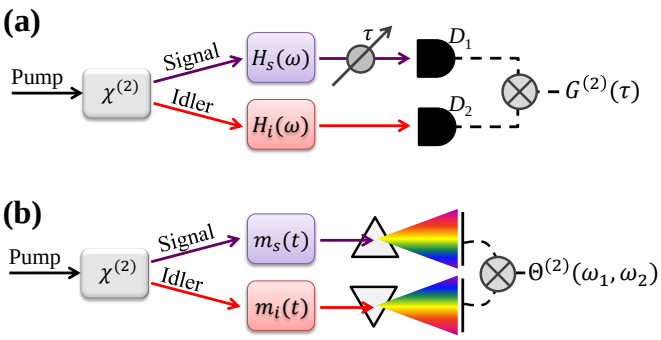

FIG. 1 Basic experimental setups for biphoton manipulation. (a) Pulse shaping. Each photon of an entangled pair is sent through a programmable spectral filter and detected on a photon counter. The coincidences between these (ideal) detectors map out the second-order Glauber correlation function $G^{(2)}(\tau)$. (b) Electro-optic modulation. The photons are now modulated in the time domain, with spectral correlations determined through coincidences between monochromators. This experiment represents the Fourier dual to that in (a).

so we can view $G^{(2)}(\tau)$ as the general quantum mechanical version of an intensity cross-correlation measurement.

When the quantum state contains no more than two phtns, $G^{(2)}(\tau)$ can be conveniently expressed as the modulus squared of a biphoton wavepacket $\psi(t+\tau, t)$, defined as (Shih, 2003)

$$\psi(t+\tau, t) = \langle\text{vac}|\hat{E}_s^{(+)}(t+\tau)\hat{E}_i^{(+)}(t)|\Psi\rangle. \quad (3)$$

For the quantum state in Eq. (1) and the setup in Fig. 1(a), the wavepacket assumes the form (Lukens *et al.*, 2013b)

$$\psi(\tau) = \int d\Omega\, \phi(\Omega)H_s(\omega_0+\Omega)H_i(\omega_0-\Omega)e^{-i\Omega\tau}, \quad (4)$$

where we have neglected an unimportant overall constant and a t-dependence which vanishes on taking the modulus $G^{(2)}(\tau) = |\psi(\tau)|^2$. This expression represents the fundamental relation for biphoton pulse shaping and well describes the spectral filtering experiments in this review. Therefore, analogous to a classical pulse (Weiner, 2011), the signal-idler temporal correlations can be shaped through programmable filtering, permitting synthesis of waveforms orders of magnitude too fast for even the speediest electronics. However, unlike the classical case, the net transfer function is the *product* of the complex filters applied to the signal and idler photons, evaluated at each entangled frequency combination. Thus the filtering applied to the signal can actually be undone by filtering the idler with the inverse; for example, even when both photons are dispersively broadened *individually*, it is possible that *collectively* their correlations remain unaltered, an effect known as nonlocal dispersion cancellation (Franson, 1992) and considered in more detail in Sec. IV.B.

The second class of experiments we examine here is essentially the Fourier dual to the pulse shaping arrangement above. A schematic of this general setup is provided in Fig. 1(b).

Now the signal and idler photons are multiplied in the time domain by the modulation functions $m_s(t)$ and $m_i(t)$, and then the spectral correlations are measured—i.e., the coincidences between two narrow frequency bins. In the absence of modulation, the entangled state in Eq. (1) indicates that only frequency pairs (ω_s, ω_i) satisfying $\omega_s+\omega_i = 2\omega_0$ will register coincidences; however, the presence of the modulators can introduce new frequency correlations, quantified by the spectral version of the Glauber correlation function:

$$\Theta^{(2)}(\omega_1, \omega_2) = \langle\Phi|\hat{\mathcal{E}}_i(-\omega_2)\hat{\mathcal{E}}_s(-\omega_1)\hat{\mathcal{E}}_s(\omega_1)\hat{\mathcal{E}}_i(\omega_2)|\Phi\rangle. \quad (5)$$

These operators are the Fourier transforms of those in Eq. (2), with negative- and positive-frequency arguments signifying photon creation and annihilation, respectively. Therefore $\Theta^{(2)}(\omega_1, \omega_2)$ is proportional to the probability of detecting a signal photon at frequency ω_1 and an idler at ω_2. Additionally, in the same fashion as the temporal case, this correlation function can be decomposed into the modulus squared of a biphoton spectral amplitude, denoted by $\theta(\omega_1, \omega_2)$:

$$\theta(\omega_1, \omega_2) = \langle\text{vac}|\hat{\mathcal{E}}_s(\omega_1)\hat{\mathcal{E}}_i(\omega_2)|\Psi\rangle. \quad (6)$$

The effect of temporal modulation is to produce convolution in the frequency domain, and in general the full expression for $\Theta^{(2)}(\omega_1, \omega_2)$ in the arrangement of Fig. 1(b) can become quite complicated. Yet if we restrict ourselves to the case in which the biphoton duration is much shorter than the scale over which the modulators vary, we can treat the inverse Fourier transform of $\phi(\Omega)$ as an impulse, giving for the biphoton spectrum

$$\theta(\Delta) = \int dt\, m_s(t) m_i(t) e^{i\Delta t}, \quad (7)$$

where we have neglected irrelevant overall constants and defined $\Delta = \omega_s + \omega_i - 2\omega_0$, the deviation of the sum frequency from that of the narrowband pump. In analogy with the spectral filtering case in Eq. (4), the effect of signal and idler modulation is cumulative, with the potential for one modulator to nonlocally cancel the other in the measured spectral correlation (Harris, 2008).

The above theory, typified in Eqs. (4) and (7), has motivated several experimental tests of Fourier-transform pulse shaping and high-speed electro-optic modulation of biphoton states—both well-established disciplines in ultrafast photonics and optical communications, but hitherto largely overlooked in the quantum optics community. Yet before delving into these experiments, we pause to discuss the key advances in ultrafast detection schemes without which many of these experiments would have proven impossible.

III. DETECTION METHODS

In the conceptual pictures of Fig. 1, we have envisioned correlating the photoelectric pulses generated from two single-photon counters in order to determine coincident photon arrivals. In the spectral measurement of Fig. 1(b), such a scheme poses no problems, for high frequency resolution is attainable with well-chosen lenses and gratings; the timing resolution of the detector is not a limiting factor. However, since most single-photon detectors suffer from timing jitters of tens of picoseconds—or more—a realistic implementation of Fig. 1(a) is unable to resolve biphoton correlations on the few- and sub-picosecond time scales. And although there are several interesting examples of shaping experiments with such slow detectors (Dayan *et al.*, 2007; Lukens *et al.*, 2013a; Poem *et al.*, 2012), the full potential of programmable pulse shaping is only realized on the ultrafast time scale. This timing resolution problem permeates classical optics as well, where correlation techniques based on nonlinear optical interactions have facilitated high-resolution temporal measurements of ultrashort pulses (Weiner, 2009). Borrowing on these ideas, one naturally hopes for a nonlinear process at the single-photon level which would likewise provide sufficient temporal resolution to characterize sub-picosecond biphoton correlations.

Such a technique has indeed been implemented: biphoton sum-frequency generation (SFG). In this process, signal and idler photons are mixed on a second nonlinear crystal; with some small probability, temporally coincident photons can then recombine and generate a photon at the sum frequency (Dayan *et al.*, 2005). Since only photons that overlap within a femtosecond timescale can mix, the rate of upconversion is proportional to the Glauber correlation function, and so by sweeping the delay of the signal with respect to the idler, $G^{(2)}(\tau)$ is directly obtained. In this way SFG enforces temporal gating optically, instead of electronically, thereby enabling orders of magnitude improvements in timing resolution.

Unfortunately, since the interacting fields have extremely low intensities, the efficiency of biphoton SFG is quite low, with a record upconversion rate of only 10^{-5} (Lukens *et al.*, 2013b). Yet such low efficiencies can be compensated by generating an ultrahigh flux of entangled photons (Dayan *et al.*, 2005). As a general rule, in order to observe quantum mechanical effects, one must ensure that only a single biphoton is created within a given detection window; otherwise, there will result spurious coincidences in which the two detections actually correspond to different photon pairs, instead of the same one. Since photons from separate pairs are not entangled, the desired quantum correlations are degraded. This limiting timescale for separate detectors—as in Fig. 1(a)—is electronic in origin, which, e.g., for 1-ns resolution fixes the maximum biphoton generation rate at $\sim 10^9$ s^{-1}. On the other hand, with ultrafast SFG which measures the biphoton directly, we need only ensure that successive biphotons *themselves* do not temporally overlap. With correlation times below 1 ps quite common, the maximum allowable quantum flux can exceed 10^{12} s^{-1}, permitting upconversion rates that are easily detectable even at such low SFG efficiencies (Dayan *et al.*, 2005). For more details regarding the conditions under which biphoton SFG accurately reproduces the Glauber correlation function, the reader is directed to the theoretical

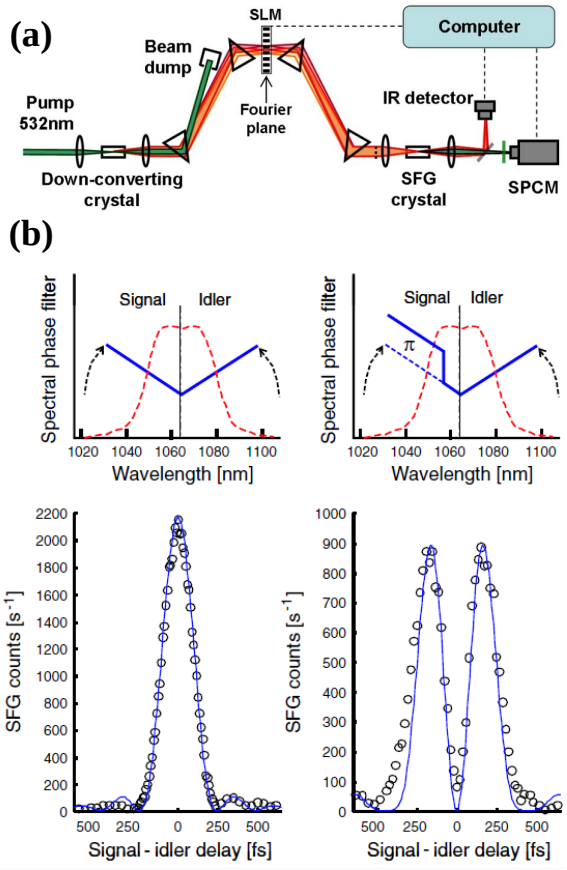

FIG. 2 First demonstration of biphoton pulse shaping. (a) Experimental setup. (b) Shaping results. In the left case, the pulse shaper sweeps the relative signal-idler delay, allowing measurement of a narrow temporal correlation function. On the right, an additional π phase shift is added halfway through the signal spectrum, turning this peak into a doublet. [Images borrowed from (Pe'er *et al.*, 2005).]

development in (Dayan, 2007).

Accordingly, the first demonstration of successful biphoton SFG (Dayan *et al.*, 2005) provided the necessary basis for biphoton pulse shaping, which itself was realized shortly thereafter (Pe'er *et al.*, 2005). The original experimental setup is reproduced in Fig. 2(a). Signal and idler photons are emitted collinearly, with a prism sequence removing remaining pump light and spectrally decomposing the biphoton; by placing a spatial light modulator (SLM) in the path of the dispersed photons, the spectral phase of the signal and idler can be programmably controlled. (Since signal and idler are distinguished by frequency, both filters can be implemented on a single pulse shaper.) The shaped biphotons are then recombined on a second nonlinear crystal, and the SFG photons are measured by a single-photon counting module (SPCM). Additionally, because a shift in time is equivalent to linear phase in the frequency domain, the pulse shaper can also impose the relative photon delay, omitting the need for a dedicated delay stage.

Figure 2(b) shows some of the results from this experiment (Pe'er *et al.*, 2005). With linear phase swept on the pulse shaper, but no filtering otherwise, a narrow correlation peak is found; by adding a π phase jump halfway through the signal spectrum, this single correlation peak is transformed into a doublet. These seminal results can be considered the foundation of biphoton pulse shaping, upon which subsequent researchers have expanded with more sophisticated filtering or efficient detection.

IV. BIPHOTON SHAPING EXPERIMENTS

A. General Overview

The first demonstration of biphoton pulse shaping (Pe'er *et al.*, 2005) utilized a relatively low-resolution, phase-only pulse shaper, and succeeding work has focused at least in part on enhancing these capabilities. In 2008, the first biphoton pulse shaper which controlled both amplitude and phase was implemented (Zäh *et al.*, 2008). One interesting consequence of independent phase and amplitude control is the ability to simulate a Franson interferometer (Franson, 1989). In the typical Franson arrangement, signal and idler photons are sent through separate Mach-Zehnder interferometers (MZIs), with coincidences recorded between one output port of each MZI. If the long-arm delay exceeds the single-photon coherence time, but not that of the original pump, the single detector rates show no interference while the coincidence rate does, due to the interference of indistinguishable quantum paths (Mandel, 1999). Yet because an MZI represents a linear, time-invariant system, it can instead be implemented in the frequency domain, by programming the associated amplitude and phase on a pulse shaper, as first demonstrated in (Zäh *et al.*, 2008), indicating a new application of biphoton shaping—namely, stable interferometer emulation.

Pulse shaping capabilities were further broadened by experiments utilizing a high-resolution, commercial telecom pulse shaper (Lukens *et al.*, 2013a). The authors were able to demonstrate complex amplitude coding for efficient verification of spectral entanglement, as well as further pulse-shaper impersonations of various interferometers. Subsequent experiments conducted with this high-resolution pulse shaper are considered in detail in the next two subsections, in which we specialize to two particularly interesting examples of programmable shaping and modulation.

B. Cancellation of Dispersion or Modulation

The possibility for nonlocal cancellation of dispersion—the spreading of broadband pulses on propagation through a medium—was mentioned briefly in Sec. II, as a consequence of the combined effects of the signal and idler spectral filters. As shown theoretically by Franson (Franson, 1992), if the signal and idler photons travel through separate media with dispersions equal in magnitude but opposite in sign, the joint correlation function is unaffected, even when the photons are arbitrarily far apart. Although some aspects of this

effect have been shown using slow electronic coincidence detection (Baek *et al.*, 2009), it was not until utilization of ultrafast biphoton SFG that dispersion cancellation could be observed on a femtosecond scale. With the variety of low-loss dispersive media available, programmable pulse shaping is in no way required to exhibit this effect; indeed, prisms alone proved sufficient in the first observation of ultrafast dispersion cancellation (O'Donnell, 2011). However, these initial experiments considered only cancellation of second-order spectral phase, whereas control of higher orders proves essential for compressing the correlations of ultrabroadband biphotons (Harris, 2007). Cancellation of such arbitrary phase is virtually impossible with standard optical media, but it is achievable with Fourier-transform pulse shaping.

To better appreciate the origins of dispersion cancellation of arbitrary orders, we specialize Eq. (4) to phase-only filters $H_s(\omega) = \exp[i\Phi_s(\omega)]$ and $H_i(\omega) = \exp[i\Phi_i(\omega)]$, expressing each phase function as a Taylor series about ω_0:

$$\Phi_{s,i}(\omega) = \sum_{n=0}^{\infty} \frac{\Phi_{s,i}^{(n)}}{n!}(\omega - \omega_0)^n. \tag{8}$$

Under these conditions, the measured biphoton wavepacket is

$$\psi(\tau) = \int d\Omega\, \phi(\Omega) \exp\left\{ -i\Omega\tau + i\sum_{n=0}^{\infty} \frac{1}{n!}\left[\Phi_s^{(n)} + (-1)^n \Phi_i^{(n)}\right]\Omega \right\}, \tag{9}$$

so that high-order dispersion cancellation is achieved whenever the signal-idler expansion coefficients satisfy $\Phi_s^{(n)} + (-1)^n\Phi_i^{(n)} = 0$ for $n = 2, 3, \ldots$. (The $n = 0, 1$ cases do not impact the overall shape of $G^{(2)}(\tau)$.) Interestingly, opposite signs of dispersion give cancellation for even orders only, as odd orders instead require identical phase coefficients to achieve compression. This behavior stands in stark contrast to dispersion compensation with classical pulses, where all orders must be flipped in the compensating medium.

Utilizing the pulse shaper from (Lukens *et al.*, 2013a), researchers have been able to verify this fascinating behavior for high-order spectral phase, making use of highly efficient periodically poled lithium niobate waveguides for both SPDC and biphoton SFG (Lukens *et al.*, 2013b). The basic setup mirrored that in Fig. 2(a), although the prism sequence was replaced by optical fiber and a fiber-pigtailed pulse shaper. The results for high-order dispersion cancellation are reproduced in Fig. 3, showing examples for the orders from $n = 2$ to $n = 5$. With the signal portion of the spectrum programmed to a particular order of spectral phase, and nothing applied to the idler, a lowered and stretched correlation function is measured (blue cases). Similarly, when the complementary phase—equal in the odd-order cases and with a sign flip in the even cases—is applied to the idler, but nothing on the signal, another dispersed wavepacket is observed (red cases). These results can be interpreted as individually spreading one photon or the other. However, when both photons are dispersed

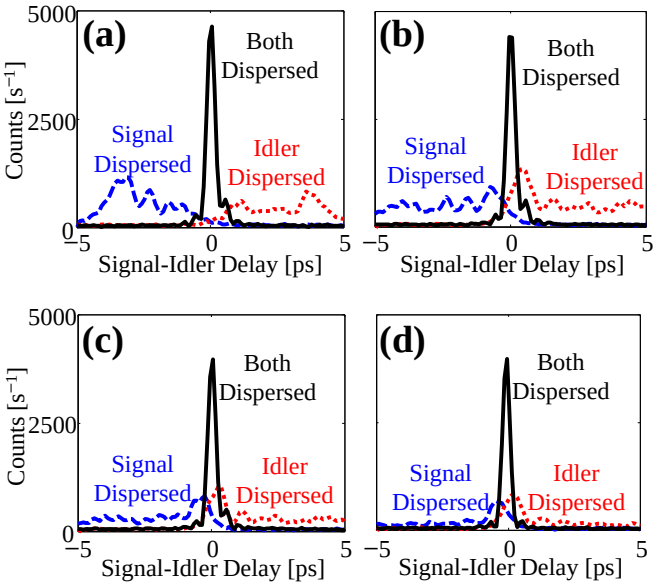

FIG. 3 High-order dispersion cancellation results for (a) second-order, (b) third-order, (c) fourth-order, and (d) fifth-order spectral phase. In all cases, dispersing both photons recovers a narrow correlation peak, whereas classical correlations would only broaden further. [Plots adapted from (Lukens *et al.*, 2013b).]

simultaneously, the original narrow correlation function is recovered, verifying complete cancellation (black cases). These pulse shaping experiments therefore not only improve understanding of arbitrary biphoton phase, but also make significant strides in the quest for single-cycle biphotons—entangled photons with correlation times equal to a single optical period (Harris, 2007)—for only through improved control of high-order dispersion will single-cycle compression be possible.

As alluded to in Sec. II, the electro-optic modulation setup of Fig. 1(b) permits realization of the Fourier dual to biphoton dispersion cancellation—namely, nonlocal modulation. Specifically, considering equi-amplitude sinusoidal phase modulation in Eq. (7), $m_s(t) = \exp[i\delta \sin\omega_m t]$ and $m_i(t) = \exp[i\delta \sin(\omega_m t + \alpha)]$, yields the complex joint spectrum

$$\theta(\Delta) = \int dt\, \exp\left\{i\delta\left[\sin\omega_m t + \sin(\omega_m t + \alpha)\right] + i\Delta t\right\}. \tag{10}$$

Thus the modulators completely cancel each other when driven out of phase ($\alpha = \pi$), invoking the rough interpretation that although each photon individually picks up new frequency content, collectively they remain correlated at the original pump frequency.

An experiment demonstrating this behavior was carried out in 2009 (Sensarn *et al.*, 2009); the key results are depicted in Fig. 4. Recalling that $\Delta = \omega_s + \omega_i - 2\omega_0$ represents the deviation of the sum frequency from the monochromatic pump, we see that with no modulators running, a sharp correlation at $\Delta = 0$ is observed, with two additional sidebands appearing when only one photon is phase modulated. Switch-

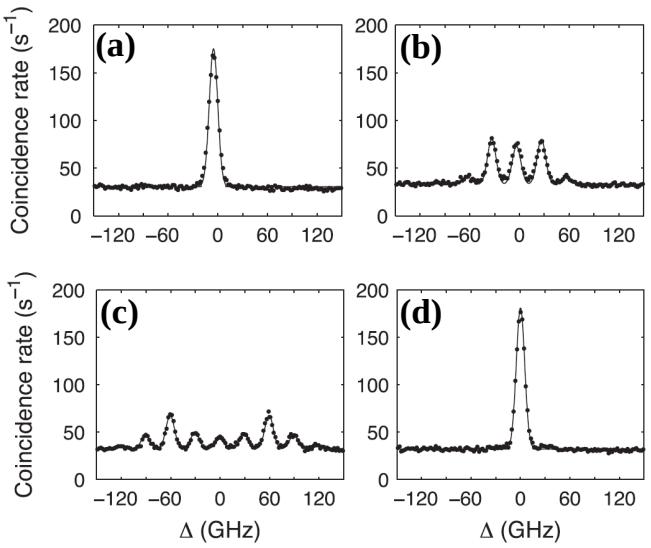

FIG. 4 Spectral correlations of temporally modulated biphotons, for (a) no modulation, (b) one photon modulated, (c) both photons modulated in phase, and (d) both photons modulated out of phase. Proper phasing allows the frequency spreading of one photon to be canceled by modulation of the other. [Results from (Sensarn *et al.*, 2009).]

ing on the second modulator in phase with the first widens the correlation bandwidth even further, whereas running the second one 180° out of phase recovers the original sharp spectral correlation, with no trace of modulation whatsoever. Taken together, these dispersion and modulation cancellation investigations provide a solid foundation for applying more complicated optical processing techniques to entangled photons, one example of which is addressed in the next section.

C. Encoding and Decoding of Biphoton Wavepackets

The previously described experiments with cancellation of polynomial spectral phase or sinusoidal temporal modulation can be viewed as building blocks for a wide range of complex coding schemes. For indeed, provided it is sufficiently well behaved, an arbitrary function can be expanded as a linear superposition of polynomials (Taylor's theorem) or sinusoids (Fourier series), implying that many alternative phase combinations could also find application in biphoton manipulation. In particular, we focus here on binary spectral or temporal phase sequences, common in optical code-division multiple-access communications (Heritage and Weiner, 2007). In the classical spectral case, a code of 0 and π phases is imposed on the frequency spectrum of an ultrashort pulse, which spreads and lowers the waveform in time; only by applying the conjugate code is the original pulse recovered, thereby allowing users with different codes to communicate over the same time-frequency space. In the Fourier dual, the phase code is temporally modulated onto a narrowband optical signal, spreading the frequency content; as before, the original narrowband message is recovered by demodulating with the correct temporal code. This latter process is an example of spread-spectrum communication, which has proven itself adept at covert transmission and jamming resistance (Pickholtz *et al.*, 1982). In this section, we describe two experiments which extend these classical communication techniques to entangled photons, showing how such quantum states can be "hidden" and "recovered" in either time or frequency.

First we consider frequency coding and time spreading, which is based on applying appropriate codes to a programmable pulse shaper. The basic idea and a proof-of-principle experiment were described in (Lukens *et al.*, 2014), in which the authors considered Walsh-Hadamard codes applied to the signal and idler photons. A given Hadamard code family consists of N length-N sequences of ones and minus-ones (or equivalently 0 and π phases) with the property than any two codes are orthogonal; that is, their inner product is zero. Examining Eq. (7), we observe that for $\phi(\Omega)$ roughly flat over signal and idler passbands, and at $\tau = 0$, the biphoton wavepacket represents nothing more than the inner product of the spectral filters $H_s(\omega)$ and $H_i(\omega)$. Therefore, if these filters are codes chosen from the same Hadamard family, matched codes will give a correlation peak, whereas mismatched codes will generate a null.

An outline of how this biphoton coding process works is provided in Fig. 5(a). The signal half-spectrum of a temporally narrow biphoton is encoded with a sequence of 0 and π phases, which spreads the correlation function and produes a null at $\tau = 0$. Then the idler is decoded by applying a second Hadamard code to the lower half of the biphoton spectrum. If the codes match in the symmetric sense, the original correlation peak is restored, but if they differ, Hadamard orthogonality ensures that the correlation function instead remains spread with a zero at $\tau = 0$. In this way the biphoton can even be encoded and decoded nonlocally, if the signal and idler are spatially separated. An experimental example with length-40 Hadamard codes is furnished in Fig. 5(b). The setup is identical to that utilized in the high-order dispersion cancellation experiments (Lukens *et al.*, 2013b). When the signal is encoded with a particular Hadamard sequence, the initially sharp correlation is temporally spread. Applying the correct idler code then retrieves the original biphoton, up to a peak reduction due to scattering losses in the pulse shaper. On the other hand, the wrong idler code yields a new, but still spread, biphoton state. These results hint at the fascinating possibilities for complex spectral coding in quantum cryptography, although there remain several key hurdles, addressed briefly in Sec. V.

An example of the Fourier dual, temporal phase coding, was demonstrated in 2010 (Belthangady *et al.*, 2010). This experiment employed much more narrowband photons than the previous examples, in order to permit fractionally large spectral spreading with gigahertz modulators. Moreover, although coding and decoding could indeed be implemented nonlocally with the arrangement of Fig. 1(b), the authors instead applied both modulators to the same photon, with the entangled partner serving merely as a trigger for coincidence counting. In this way the signal photon is first temporally encoded with

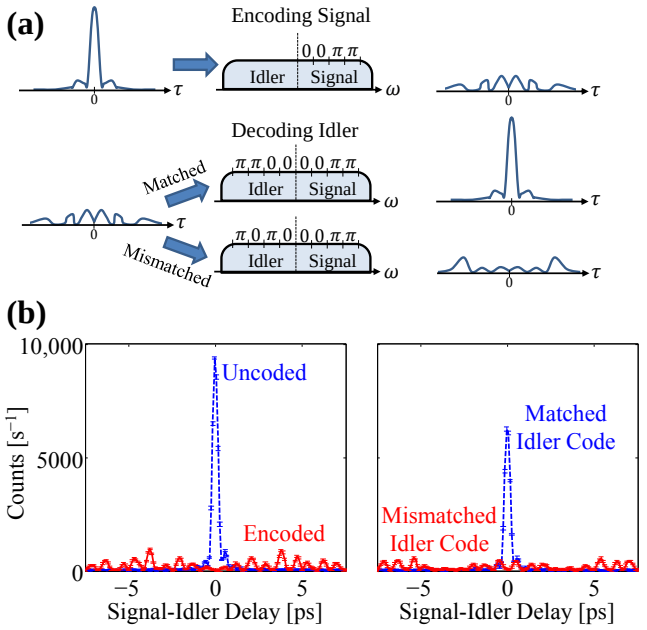

FIG. 5 Orthogonal spectral coding of entangled photons. (a) Schematic of the basic process, in which the signal photon is encoded and the idler decoded; only when the codes match is the ultrashort biphoton correlation recovered. (b) Experimental results for length-40 Hadamard codes, confirming the conceptual picture in (a). [Images adapted from (Lukens *et al.*, 2014).]

a pseudorandom sequence of $\pm\pi/2$ phases, which frequency spreads the 3.5-MHz photon to around 10 GHz. Then a second modulator is applied, followed by a narrowband filter, before detection. To guarantee a high probability of transmission, the second modulator must undo the effects of the first one and restore the narrow photon spectrum; otherwise, the filter will most likely reject the frequency-spread photon. This provides an interesting way to hide single photons.

To demonstrate this capability, the authors injected a laser field at the same frequency and with flux over $1000\times$ that of the original photon, after the first modulator but before the second. As shown in Fig. 6(a), when both modulators are turned off, the laser field dominates the coincidence counts, with no evidence of time correlation. But when the modulators are turned on, the shape of the hidden single photon is found [Fig. 6(b)]. This ensues because the photon is frequency spread by the first modulator and despread by the second, thereby passing through the narrowband detection filter with ease; on the other hand, the laser is transformed only by the second modulator, so its spectrum is spread right before the filter and is therefore highly attenuated. As this experiment highlights, even the thoroughly classical concept of spread spectrum can be applied to single-photon signals.

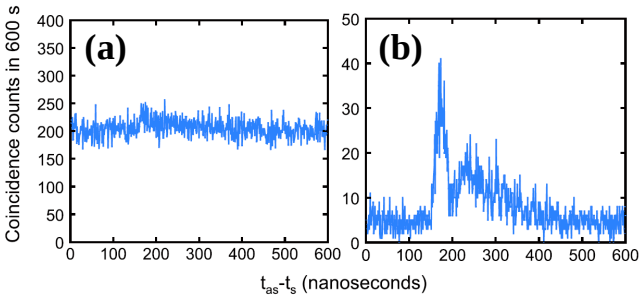

FIG. 6 Hiding single photons. (a) With no temporal modulation, the single-photon field is completely hidden by a much more powerful laser beam. (b) But when a temporal encoding and decoding process analagous to classical spread spectrum is applied, the uncoded laser is rejected and the characteristic shape of the single photon is recovered. [Results borrowed from (Belthangady *et al.*, 2010).]

V. OUTLOOK

The examples of biphoton pulse shaping and modulation considered in this review indicate the rapid development of this field, which over the last decade has succeeded in combining these classical technologies with quantum states of light. Nonetheless, there remain several important avenues of research to bring these proof-of-principle experiments to more applied specializations, such as secure quantum key distribution (QKD). In some ways SFG, which proved essential in the above demonstrations of biphoton pulse shaping, now sits as a hindrance to further development. For by requiring signal-idler recombination, any experiments utilizing biphoton SFG are intrinsically ill-suited for QKD implementations, in which the two communicating parties must obviously be spatially separated for any useful application. It is therefore desirable to find alternative high-time-resolution detection methods which could observe these effects nonlocally. Pending further improvements in single-photon detector jitter to the picosecond level (Hadfield, 2009), methods based on single-photon mixing with ultrashort (Kuzucu *et al.*, 2008) or chirped (Donohue *et al.*, 2013) classical pulses seem particularly promising, and so nonlocal generalizations of ultrafast dispersion cancellation and orthogonal coding may be possible with such techniques, although they have yet to be demonstrated. Moreover, high-dimensional time-frequency QKD protocols based on dispersion (Mower *et al.*, 2013) or temporal modulation (Nunn *et al.*, 2013) have recently been proposed, and it would be interesting to investigate how sophisticated biphoton control could be exploited to realize these schemes in practice.

So while experiments up to this point have already revealed new insights into the behavior of entangled photons, numerous opportunities remain unexplored. Thus we expect the next decade to witness even more advances in biphoton pulse shaping; we have only begun to scratch the surface of the potential contained in such entangled quanta, and technologies developed in classical optics will no doubt continue to find unanticipated uses in the quantum regime.

REFERENCES

Aspect, A. (1999), Nature **398**, 189.

Baek, S.-Y., Y.-W. Cho, and Y.-H. Kim (2009), Opt. Express **17**, 19241.

Belthangady, C., C.-S. Chuu, I. A. Yu, G. Y. Yin, J. M. Kahn, and S. E. Harris (2010), Phys. Rev. Lett. **104**, 223601.

Brannen, E., and H. I. S. Fergusen (1956), Nature **178**, 481.

Chekhova, M. (2011), Ch. 4 of *Progress in Optics,* Vol. 56, (ed. E. Wolf).

Dayan, B. (2007), Phys. Rev. A **76**, 043813.

Dayan, B., Y. Bromberg, I. Afek, and Y. Silberberg (2007), Phys. Rev. A **75**, 043804.

Dayan, B., A. Pe'er, A. A. Friesem, and Y. Silberberg (2005), Phys. Rev. Lett. **94**, 043602.

Donohue, J. M., M. Agnew, J. Lavoie, and K. J. Resch (2013), Phys. Rev. Lett. **111**, 153602.

Einstein, A., B. Podolsky, and N. Rosen (1935), Phys. Rev. **47**, 777.

Fellgett, P. (1957), Nature **179**, 956.

Franson, J. D. (1989), Phys. Rev. Lett. **62**, 2205.

Franson, J. D. (1992), Phys. Rev. A **45**, 3126.

Gisin, N., G. Ribordy, W. Tittel, and H. Zbinden (2002), Rev. Mod. Phys. **74**, 145.

Glauber, R. J. (1963a), Phys. Rev. **130**, 2529.

Glauber, R. J. (1963b), Phys. Rev. **131**, 2766.

Hadfield, R. H. (2009), Nat. Photon. **3**, 696.

Hanbury Brown, R., and R. Q. Twiss (1956a), Nature **177**, 27.

Hanbury Brown, R., and R. Q. Twiss (1956b), Nature **178**, 1447.

Hanbury Brown, R., and R. Q. Twiss (1956c), Nature **178**, 1046.

Harris, S. E. (2007), Phys. Rev. Lett. **98**, 063602.

Harris, S. E. (2008), Phys. Rev. A **78**, 021807.

Heritage, J. P., and A. M. Weiner (2007), IEEE J. Sel. Top. Quantum Elec. **13**, 1351.

Kuzucu, O., F. N. C. Wong, S. Kurimura, and S. Tovstonog (2008), Phys. Rev. Lett. **101**, 153602.

Lukens, J. M., A. Dezfooliyan, C. Langrock, M. M. Fejer, D. E. Leaird, and A. M. Weiner (2013a), Opt. Lett. **38**, 4652.

Lukens, J. M., A. Dezfooliyan, C. Langrock, M. M. Fejer, D. E. Leaird, and A. M. Weiner (2013b), Phys. Rev. Lett. **111**, 193603.

Lukens, J. M., A. Dezfooliyan, C. Langrock, M. M. Fejer, D. E. Leaird, and A. M. Weiner (2014), Phys. Rev. Lett. **112**, 133602.

Mandel, L. (1999), Rev. Mod. Phys. **71**, S274.

Mandel, L., and E. Wolf (1995), *Optical Coherence and Quantum Optics* (Cambridge University Press, Cambridge, UK).

Mower, J., Z. Zhang, P. Desjardins, C. Lee, J. H. Shapiro, and D. Englund (2013), Phys. Rev. A **87**, 062322.

Nunn, J., L. J. Wright, C. Söller, L. Zhang, I. A. Walmsley, and B. J. Smith (2013), Opt. Express **21**, 15959.

O'Donnell, K. A. (2011), Phys. Rev. Lett. **106**, 063601.

Pe'er, A., B. Dayan, A. A. Friesem, and Y. Silberberg (2005), Phys. Rev. Lett. **94**, 073601.

Pickholtz, R., D. Schilling, and L. Milstein (1982), IEEE Trans. Commun. **30**, 855.

Poem, E., Y. Gilead, Y. Lahini, and Y. Silberberg (2012), Phys. Rev. A **86**, 023836.

Purcell, E. M. (1956), Nature **178**, 1449.

Sensarn, S., G. Y. Yin, and S. E. Harris (2009), Phys. Rev. Lett. **103**, 163601.

Shih, Y. (2003), Rep. Prog. Phys. **66**, 1009.

Weiner, A. M. (2009), *Ultrafast Optics* (Wiley, Hoboken, NJ).

Weiner, A. M. (2011), Opt. Commun. **284**, 3669.

Zäh, F., M. Halder, and T. Feurer (2008), Opt. Express **16**, 16452.